E. Ghanaee, J. I. Pérez-Díaz, D. Fernández-Muñoz, J. Nájera and M. Chazarra, "Comparative Analysis of Battery Degradation Models for Optimal Operation of a Hybrid Power Plant in the Day-Ahead Market," 2025 IEEE Kiel PowerTech, Kiel, Germany, 2025, pp. 1-6, doi: 10.1109/PowerTech59965.2025.11180334.

Comparative Analysis of Battery Degradation Models for Optimal Operation of a Hybrid Power Plant in the Day-Ahead Energy Market

Elahe Ghanaee
ETSI Caminos, Canales y Puertos
Universidad Politécnica de Madrid
Madrid, Spain
elahe.ghanaee@upm.es

Juan Ignacio Pérez-Díaz
ETSI Caminos, Canales y Puertos
Universidad Politécnica de Madrid
Madrid, Spain
ji.perez@upm.es

Daniel Fernández-Muñoz
ETSI Telecomunicación
Universidad Politécnica de Madrid
Madrid, Spain
daniel.fernandezm@upm.es

Jorge Nájera
Unidad de Accionamientos Eléctricos
CIEMAT
Madrid, Spain
jorge.najera@ciemat.es

Manuel Chazarra
ETSI Caminos, Canales y Puertos
Universidad Politécnica de Madrid
Madrid, Spain
manuel.chazarra@upm.es

***Abstract*—Battery degradation significantly impacts the operational costs and profitability of hybrid power plants (HPPs) participating in the day-ahead (DA) energy market. This paper conducts a comparative analysis of the effectiveness of three battery degradation models. The models calculate the battery degradation as a function of the energy throughput (TP model), the discharge maneuvers (DM model) and based on the Rainflow cycle counting algorithm (RF model). A deterministic mixed-integer linear programming model is developed to maximize revenue of HPPs participating in the DA market considering battery degradation costs. Numerical results reveal that the TP model provides the highest profitability in the DA energy market with the lowest computational complexity, while the RF and DM models capture the battery aging with higher accuracy. This comparative analysis offers some insights useful for selecting appropriate degradation models for better operational performance and longer battery life.**

***Index Terms*—Hybrid power plant, DA energy market, battery degradation, cycle aging**

NOMENCLATURE

Indexes

j	Depth of discharge segments.
t	Hourly periods of the planning horizon.

Parameters

$\overline{P}^{B}$	Battery output/input power capacity [MW].
$\overline{P}^{W}$	Installed capacity of wind farm [MW].
$\overline{P}^{G}$	Grid access capacity at the point of common coupling in generation mode[MW].
$\overline{P}^{C}$	Grid access capacity at the point of common coupling in consumption mode [MW].
C^{TP}	Throughput cost [€/MWh].
λ_t^{DA}	Day-ahead energy market price in period t [€/MWh].
η^{B}	Total round-trip battery efficiency.
$\overline{SoC}/\underline{SoC}$	Maximum/minimum state of charge of battery [MWh].
$\overline{E}^{B}$	Battery capacity [MWh].
ω_j	Degradation cost corresponding to the depth of discharge of battery in segment j.
$\overline{\beta}_j/\underline{\beta}_j$	Maximum/minimum depth of discharge of battery in segment j.
M	A big positive constant.

Variables

p_t^{B}	Battery discharge/charge output/input power in the day-ahead energy market in the period t [MWh] (positive discharge: negative charge).
p_t^{W}	Wind energy generation in period t [MWh].
$p_t^{W,B}$	Available wind energy generation used to charge battery in period t [MWh].
$e^{B,ch}/e^{B,dch}$	Battery energy charge/discharge in period t [MWh].
DoD_t	Depth of discharge of battery in period t [MWh].
SoC_t	Battery state of charge in period t [MWh].
c^{AG}	Degradation cost [€].
$c_t^{AG,RF}$	Degradation cost of the Battery associated with RF model [€].
$c_t^{AG,Peak}$	Degradation cost of the Battery associated with a peak in period t [€].
$cp_t^{AG,Peak}$	Bilinear variable for degradation cost of battery associated with a peak in period t [€].
$c_t^{AG,Valley}$	Degradation cost of battery associated with a valley in period t [€].

$cv_t^{AG,Valley}$ Bilinear variable for degradation cost of battery associated with a valley in period t [€].

Binary Variables

$y_{t,j}$ Binary variable used for selecting battery degradation cost segment j in period t.

U_t^{dch} Binary variable corresponding to the discharging status of the battery in period t.

U_t^{Peak} Binary variable corresponding to the peak in the state of charge profile of battery.

U_t^{Valley} Binary variable corresponding to the valley in the state of charge profile of battery.

I. Introduction

The drive to decarbonize the power sector has resulted in a considerable increase in the adoption of renewable energy sources (RES), such as wind and solar power, over recent decades. However, the widespread integration of these resources has introduced significant challenges in the operation of power systems, primarily due to their inherent intermittency and variability [1]. Li-ion batteries (LIBs) are widely used in energy storage systems for the main power grid due to their high energy density. However, one of the main challenges with LIBs is degradation over time, caused by irreversible physical and chemical changes. Battery degradation is commonly studied using three types of models: physics-based [2], [3], semi-empirical [4], [5], and empirical [6]. Physics-based models use mathematical equations to describe the physical and chemical processes that cause battery aging [7]. Empirical models, on the other hand, rely on experimental data and statistical techniques to analyze degradation trends [8], [9]. As the battery ages, its performance declines, and it becomes less capable of efficiently storing and delivering energy [10]. This requires the development of a reliable battery degradation model that can accurately quantify battery degradation and be effectively integrated in the optimization model used for energy scheduling in the day-ahead (DA) market. This integration is essential for optimizing the performance of energy storage systems and ensuring their long-term viability. Modeling battery degradation is a complex process, as it arises from a combination of various mechanisms and their interactions. Numerous studies have addressed this challenge in the scientific literature. These efforts employ models that range in computational complexity, striking a balance between accuracy and practicality. To account for battery degradation in optimization frameworks, researchers typically rely on a few common approaches. These include setting direct limits on how the battery operates, such as restricting its depth of discharge or charge rates [11] , using the energy throughput method [12]–[14], approximations of the Rainflow cycle counting algorithm [15], discharging maneuvers [5] and nonlinear models [16], [17]. Nonlinear optimization models are often computationally complex while the global optimality is not guaranteed. In [12], the authors focus on energy throughput-based approaches to characterize battery degradation for investigating the impact of battery degradation on its profitability in energy arbitrage applications. The authors of Ref. [4] propose a mixed-integer linear programming (MILP) model to approximate the Rainflow cycle counting algorithm for integration into the energy scheduling of a battery energy storage system (BESS). The framework quantifies degradation costs by employing a linear representation of aging effects associated with complete and incomplete cycles. The authors of Ref. [5], develops an optimization model for the scheduling of virtual power plants, focusing on the degradation costs of LIBs, modeled based on the depth of discharge and the discharge rate.

This paper introduces three battery degradation models for integration into the short-term scheduling of a hybrid power plant (HPP) participating in the DA energy market. The study aims to analyze the impact of degradation model complexity on the revenue and net profit of the HPP within the DA energy market. Furthermore, we compare degradation costs derived from the optimization process with those obtained through post-processing state of charge (SoC) profiles of the battery using the Rainflow cycle counting algorithm. Additionally, the study evaluates the trade-offs between model complexity, computational efficiency and performance for practical use in DA market operations.

The remaining of the paper is organized as follows. Section II presents the optimization modeling. Section III introduces the battery degradation models. The application of the battery degradation model to an HPP is presented in Section IV and finally, Section V concludes the paper.

II. OPTIMIZATIOM MODELING

The short-term self-scheduling problem of an HPP participating in the Spanish DA market is formulated as a deterministic mixed integer linear program. The objective function of the optimization model is to maximize the profitability of the HPP while considering the degradation cost of battery (1).

$$\text{Max} \sum_{t=1}^{24} \left\{ \lambda_t^{DA} \times \left(p_t^W + e_t^{B,dch} - e_t^{B,ch} \right) - c_t^{AG} \right\} \quad (1)$$

The first term of the objective function represents the net revenue in the DA energy market from wind energy generation and the charging/discharging output of the battery. The last term corresponds to the degradation cost of battery due to cycle aging. The objective function is subject to constraints (3)-(9), and to the constraints presented in the next section to model the battery degradation.

$$p_t^W + p_t^{W,B} \leq \overline{P}^W \quad (2)$$

$$e_t^{B,ch} + p_t^{W,B} \leq \overline{P}^B \times (1 - U_t^{dch}) \quad (3)$$

$$e_t^{B,dch} \leq \overline{P}^B \times U_t^{dch} \quad (4)$$

$$e_t^{B,dch} - e_t^{B,ch} - p_t^{W,B} = p_t^B \quad (5)$$

$$SoC_t = SoC_{t-1} + e_t^{B,ch} \times \eta^B + p_t^{W,B} \times \eta^B - e_t^{B,dch} \quad (6)$$

$$\underline{SoC}_t \leq SoC_t \leq \overline{SoC}_t \tag{7}$$

$$p_t^W + e_t^{B,dch} - e_t^{B,ch} \leq \overline{P}^G \tag{8}$$

$$p_t^W + e_t^{B,dch} - e_t^{B,ch} \geq -\overline{P}^C \tag{9}$$

The allocation of wind energy in the DA energy market is determined using (2). The optimization model can incorporate some of the available wind energy generation to charge the battery ($p_t^{W,B}$). Constraints (3) to (5) determine the limits on the energy scheduling of battery within the DA energy market and ensure that battery energy schedule is set to either discharge or charge mode only. The SoC of the battery over a period t is described by constraints (6) and (7). The power exchanged with the grid is limited by the grid access capacity at the point of common coupling in both generation and consumption modes, as specified in (8) and (9).

III. BATTERY DEGRADATION MODELS

In this section, we compare three battery degradation models. The first degradation model (hereinafter referred to as TP model) estimates the degradation as a function of the total energy throughput. The second model (hereinafter referred to as RF model) estimates the degradation based on [1] where the authors propose an MILP formulation to approximate the Rainflow-counting algorithm. The third model (hereinafter referred to as DM model) estimates the degradation as a function of the depth of energy discharge maneuvers.

These models are incorporated into the self-scheduling problem of an HPP participating in the Spanish DA energy market. The problem is formulated as a deterministic MILP model with a 24-hour scheduling horizon, aiming to maximizing the revenue in the DA energy market accounting for battery degradation costs.

The process of determining the degradation costs of the battery in the DM model and RF model consists of three major steps. Firstly, we employ the curve shown in [18], which describes the relationship between the DoD and the total number of cycles that the battery can complete at each DoD before its capacity declines to less than 80% of its initial capacity. Secondly, the degradation cost is calculated by dividing the capital expenditure of the battery by the number of cycles corresponding to each DoD; resulting in a curve presenting a relationship between the DoD and the associated degradation cost. Finally, since the resulting curve is nonlinear, we use a stepwise linearization method to approximate it as a linear function.

A. Energy Throughput model (TP model)

The Energy Throughput model is a battery degradation model based on the concept that battery degradation is linked to the energy throughput, representing the total energy charged and discharged from the battery. This model does not incorporate additional stress factors associated with cycle aging. Degradation cost (10) is calculated based on the energy throughput of the battery and the number of full equivalent cycles the battery can perform before reaching its end of life [3].

$$c_t^{AG} = C^{TP} \times \left(p_t^{W,B} + e_t^{B,dch} + e_t^{B,ch}\right) \tag{10}$$

B. Rainflow-based cycle counting model (RF model)

In this model, the linearized Rainflow cycle counting algorithm proposed in [15] is integrated into the optimization model. The proposed algorithm identifies complete and incomplete cycles from the peaks and valleys of the SoC profile in a similar (but not the same) way to the Rainflow cycle counting algorithm.

$$DoD_t = 1 - \frac{SoC_t}{\overline{E}^B} \tag{11}$$

$$\sum_j \underline{\beta}_n \times y_{t,j} \leq DoD_t \leq \sum_j \overline{\beta}_n \times y_{t,j} \tag{12}$$

$$\sum y_{t,j} \leq 1 \tag{13}$$

$$c_t^{AG,RF} = \sum_j y_{t,j} \times \omega_j \tag{14}$$

$$U_t^{Peak} - U_t^{Valley} = U_{t+1}^{dch} - U_t^{dch} \tag{15}$$

$$U_t^{Peak} + U_t^{Valley} \leq 1 \tag{16}$$

$$c_t^{AG,Peak} = c_t^{AG,RF} \times U_t^{Peak} \tag{17}$$

$$c_t^{AG,Valley} = c_t^{AG,RF} \times U_t^{Valley} \tag{18}$$

The degradation cost associated with the life loss due to cycle aging can be calculated as the summation over t of the difference between the cost due to life loss occurring at valleys ($c_t^{AG,Valley}$) and at peaks ($c_t^{AG,Peak}$) in the SoC profile of the battery.

The amount of DoD for the specified period t is delineated by equation (11). Constraint (12) identifies the chosen segment of the DoD and ensures that the binary variable ($y_{t,j}$) corresponding to the jth segment of DoD will equal 1 or 0 , consistently. Constraint (13) ensures that in each period t, only one segment is chosen. In (14), the degradation cost corresponding to the chosen segment of DoD is calculated.

According to constraint (15) and (16), the peaks and valleys in each period t can be identified and assigned exclusively as either a peak or a valley. When the battery begins the discharge process, it identifies a peak, and the binary variable (U_t^{Peak}) takes the value of 1. Conversely, once the discharging process of the battery is complete, a valley is identified, and the binary variable (U_t^{Valley}) will equal 1. Constraints (17) and (18) determine the cost associated with the peak and valley in the period t.

It is important to highlight that the non-linear term on the right-hand side of constraint (17) and (18), which involves the multiplication of the binary variables (U_t^{Peak}) and (U_t^{Valley}) and the continuous variable ($c_t^{AG,RF}$), can be substituted with new bilinear variables (cp_t^{AG}) and (cv_t^{AG}), respectively, along

with constraints (19) to (24) where M represents a big positive constant.

$$cp_t^{AG} \leq M \times U_t^{Peak} \tag{19}$$

$$cp_t^{AG} \leq c_t^{AG,RF} + M \times (1 - U_t^{Peak}) \tag{20}$$

$$cp_t^{AG} \geq c_t^{AG,RF} - M \times (1 - U_t^{Peak}) \tag{21}$$

$$cv_t^{AG} \leq M \times U_t^{Valley} \tag{22}$$

$$cv_t^{AG} \leq c_t^{AG,RF} + M \times (1 - U_t^{Valley}) \tag{23}$$

$$cp_t^{AG} \geq c_t^{AG,RF} - M \times (1 - U_t^{Valley}) \tag{24}$$

$$c_t^{AG} = (cv_t^{AG} - cp_t^{AG}) \tag{25}$$

C. Discharge maneuvers model (DM model)

This model distinguishes battery degradation cost based on the DoD of battery [5]. The battery degradation cost for each discharge maneuver is calculated based on the same curve that was described at the beginning of this section.

$$DoD_t \geq \frac{SoC_{t-1} - SoC_t}{\overline{E}^B} \tag{26}$$

$$\sum_j \underline{\beta}_n \times y_{t,j} \leq DoD_t \leq \sum_j \overline{\beta}_n \times y_{t,j} \tag{27}$$

$$\sum y_{t,j} \leq 1 \tag{28}$$

$$c_t^{AG} = \sum_j y_{t,j} \times \omega_j \tag{29}$$

The DoD for the period t is represented by (26). Constraint (27) defines the selected segment of the DoD and specifies that the binary variable $(y_{t,j})$ corresponding to the segment jth of DoD will take a value of 1. Constraint (27) ensures that in each period t, only one segment is selected. Constraint (29) computes the degradation cost due to the discharging of battery in the jth segment of DoD.

IV. CASE STUDY

The HPP considered in this section features a LIB with 2 MW power output/input capacity, a storage capacity of 4 MWh, and a wind farm with a total installed capacity of 4.5 MW.

A. Data

In the Spanish DA market the bids must be submitted 14 to 38 hours before the operation settlement period. The gate closure time of the market is noon. Since most of the energy is negotiated in the DA market, this market has the highest liquidity [19].

A set of 32 scenarios is used as input to the short-term scheduling model to get enough representative results on the performance of the model. Each scenario comprises the following data series (each spanning 24 hours): (i) DA electricity market price, and (ii) forecast wind generation. The scenarios for the DA energy market prices are provided in [20].

B. Numerical Results

The deterministic MILP model is executed using the CPLEX commercial solver through GAMS.

In this subsection, we analyze and compare the HPP's scheduling decisions, total revenue and profit in the DA market, and the degradation costs derived from the optimization and post-processing the SoC profile of battery through the Rainflow cycle counting algorithm.

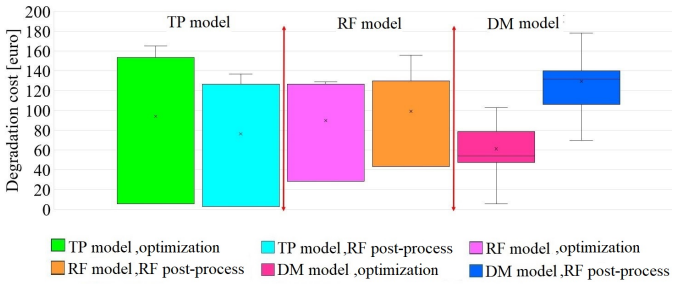

Fig. 1. Boxplot of degradation costs for the three models derived from the optimization and by post-processing (Rainflow) SoC profiles of battery across the 32 scenarios.

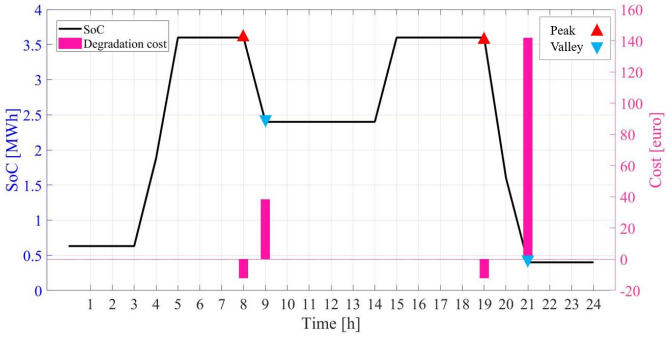

Fig. 2. SoC profile, peaks and valleys and the corresponded degradation costs obtained by the RF model in one of the scenarios.

TABLE I
RESULTS OF RAIN FLOW CYCLE COUNTING ALGORITHM FOR A SINGLE DAY SCENARIO OF SOC PROFILE

Cycles	Start Point of Cycle	End Point of Cycle	Depth of Cycle [p.u]	Cycle Cost [€]
Full cycle	5	9	0.3	32.2
Half cycle	0	15	0.74	59.4
Half cycle	15	24	0.8	67.1

Fig. 1 compares the degradation costs obtained from the results of the optimization model and by post-processing the SoC profile of battery through the Rainflow cycle counting algorithm for the three models considered. According to this figure, the DM model provides the lowest average degradation cost, followed by the RF model and the TP model. In contrast, after post-processing the SoC profiles of battery, it is revealed that the DM model has the highest average degradation cost, while the TP model has the lowest one.

Additionally, it can be observed that although the RF model is based on the Rainflow-counting algorithm, there is a 9% difference between the average cost calculated by the optimization problem and the cost computed after post-processing the SoC profiles across the 32 scenarios. This can be explained from Fig. 2, which illustrates the SoC profile, peaks and valleys obtained by the RF model in one of the 32 scenarios. As can be seen in the figure the RF model identifies a peak and a valley at hours 8 and 9, as well as another peak and valley at hours 19 and 21. According to RF model, whenever the battery discharging process begins, a peak is identified, and a valley is observed when the process ends, as shown in the figure. The degradation costs associated with the peaks and valleys are also depicted in the figure. The degradation cost corresponds to the summation over t of the difference between the cost at valleys and the cost at peaks.

However, when one post-processes the SoC profile through the Rainflow cycle counting algorithm, as shown in Table I, one full cycle and two half cycles are identified in the SoC profile. The table shows the cost associated with each cycle, with a total degradation cost of 158.79 euros, which is 32.25 euros higher than the degradation cost obtained from the optimization (126.54 euros). Therefore, it becomes clear that this model is not fully consistent with the Rainflow cycle counting algorithm.

Fig. 3 presents the average revenue and profit of the HPP in the DA market across the 32 scenarios for the three models. As illustrated, the DM model yields the highest revenue, followed by the RF model and TP model. However, the TP model achieves the highest profit in the DA market, while the DM model results in the lowest profit. The profit in the DA market is determined as the total revenue in the DA market obtained through optimization minus the battery degradation cost computed by post-processing the SoC profile through the Rainflow cycle counting algorithm.

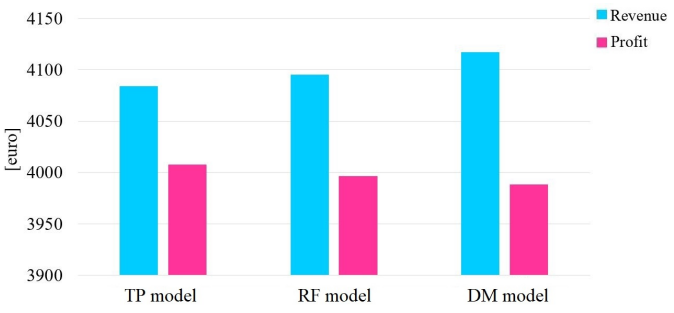

Fig. 3. Average revenue and profit of the HPP in the DA market across.

Fig. 4 compares the loss of life obtained with three analyzed models after post-processing across the 32 scenarios. The DM model shows the highest average loss of life, which is 68.6% and 43.4% greater than that of the TP model and RF model, respectively.

Table II shows the dimensions of the optimization models for the three models. According to the table, the RF model is the most complex model. Given that the size of the optimization model significantly influences the computational time, the TP model is the fastest model, while the RF model is the slowest. Although the DM model has a considerably larger dimension compared to the TP model, it is only slightly slower in terms of computational time.

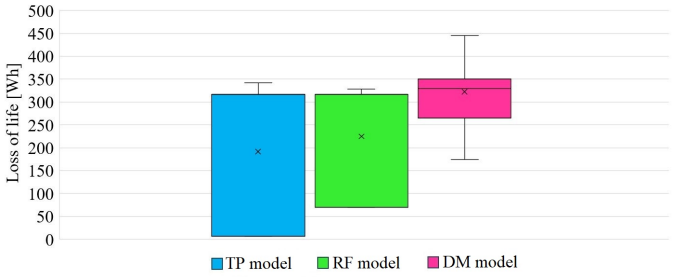

Fig. 4. Boxplot of loss of life computed by post-processing the SoC profile through the Rainflow cycle counting algorithm across the 32 scenarios.

TABLE II
DIMENSIONS OF THE OPTIMIZATION PROBLEM

	TP model	**RF model**	**DM model**
Numbers of constraints	169	601	289
Numbers of continuous variables	145	265	193
Numbers of binary variables	24	336	264
Average computational time [s]	0.064	108.06	0.073

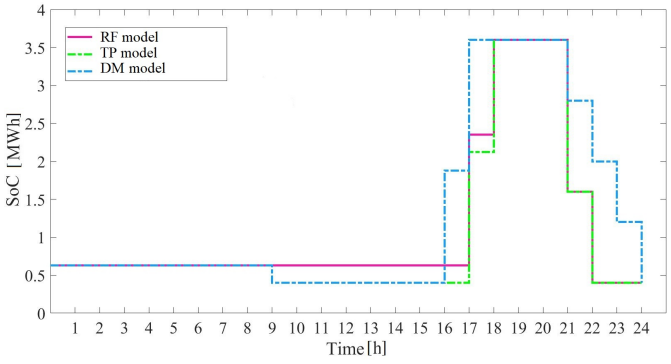

Fig. 5. SoC of the battery for a single scenario.

Fig. 5 illustrates the SoC of battery for a single scenario. As observed, the DM model maintains a higher SoC level for most of the day, while the TP model shows the lowest SoC levels. This may have an impact on the battery calendar aging. Its consideration is out of the scope of the current paper but will soon be addressed in future works.

V. CONCLUSION

This study presented a detailed comparative analysis of three battery degradation models used for the energy scheduling of an HPP in the DA market. The models calculate the battery degradation as a function of the energy throughput (TP model), the depth of the energy discharge maneuvers (DM model), and based on a linear approximation of the Rainflow cycle counting algorithm (RF model). The results show large differences in degradation costs, computational complexity, and overall profitability among the models. Although the RF model is based on the Rainflow cycle counting algorithm, it shows a 9% difference between the degradation cost obtained as result of the optimization and that calculated by post-processing the SoC profile through the Rainflow cycle counting algorithm, in addition to requiring more computational time. On the other hand, the TP model, though less accurate, provides the highest profit with the lowest computational time. In addition, the DM model yields the highest revenue while the lowest profit in the DA market. The present study points out the importance of selecting adequate degradation models according to specific operational and computational needs to increase profitability and battery life time.

ACKNOWLEDGMENT

This work has been financed by MICIU/AEI/10.13039/501100011033/ Unión Europea NextGenerationEU/PRTR through Project TED2021-132794B-C211.

REFERENCES

[1] Q. Li, J. Wang, Y. Zhang, Q. Wu, C. Gu, and Q. Yang, "Hierarchical market-based optimal planning of transmission network and wind-storage hybrid power plant," *International Journal of Electrical Power & Energy Systems*, vol. 153, p. 109328, 2023.

[2] E. Hasani, F. Torabi, and A. Salavati-Zadeh, "Electrochemical simulation of lithium-ion batteries: a novel computational approach for optimizing performance," *Hydrogen, Fuel Cell & Energy Storage*, vol. 11, no. 4, pp. 215–224, 2024.

[3] N. Collath, M. Cornejo, V. Engwerth, H. Hesse, and A. Jossen, "Increasing the lifetime profitability of battery energy storage systems through aging aware operation," *Applied Energy*, vol. 348, p. 121531, 2023.

[4] M. Amini, M. H. Nazari, and S. H. Hosseinian, "Predictive energy management strategy for battery energy storage considering battery degradation cost," *IET Renewable Power Generation*, vol. 17, no. 5, pp. 1119–1138, 2023.

[5] D. Fernández-Muñoz and J. I. Pérez-Díaz, "Optimisation models for the day-ahead energy and reserve self-scheduling of a hybrid wind–battery virtual power plant," *Journal of Energy Storage*, vol. 57, p. 106296, 2023.

[6] M. Petit, E. Prada, and V. Sauvant-Moynot, "Development of an empirical aging model for li-ion batteries and application to assess the impact of vehicle-to-grid strategies on battery lifetime," *Applied Energy*, vol. 172, pp. 398–407, 2016.

[7] G. Ning and B. Popov, "Cycle life modeling of lithium-ion batteries," *Journal of The Electrochemical Society - J ELECTROCHEM SOC*, vol. 151, pp. 1584–1591, 01 2004.

[8] S. Nazaralizadeh, P. Banerjee, A. K. Srivastava, and P. Famouri, "Battery energy storage systems: A review of energy management systems and health metrics," *Energies*, vol. 17, no. 5, 2024.

[9] D. B. S. Oliveira, L. L. Glória, R. A. S. Kraemer, A. C. Silva, D. P. Dias, A. C. Oliveira, M. A. I. Martins, M. A. Ludwig, V. F. Gruner, L. Schmitz, and R. F. Coelho, "Mixed-integer linear programming model to assess lithium-ion battery degradation cost," *Energies*, vol. 15, no. 9, 2022.

[10] J. Li, R. Landers, and J. Park, "A comprehensive single-particle-degradation model for battery state-of-health prediction," *Journal of Power Sources*, vol. 456, p. 227950, 2020.

[11] X. Huang, Q. Huang, H. Cao, Q. Wang, W. Yan, and L. Cao, "Battery capacity selection for electric construction machinery considering variable operating conditions and multiple interest claims," *Energy*, vol. 275, p. 127454, 2023.

[12] F. Wankmüller, P. R. Thimmapuram, K. G. Gallagher, and A. Botterud, "Impact of battery degradation on energy arbitrage revenue of grid-level energy storage," *Journal of Energy Storage*, vol. 10, pp. 56–66, 2017.

[13] M. Zheng, C. J. Meinrenken, and K. S. Lackner, "Smart households: Dispatch strategies and economic analysis of distributed energy storage for residential peak shaving," *Applied Energy*, vol. 147, pp. 246–257, 2015.

[14] B. Xu, "The role of modeling battery degradation in bulk power system optimizations," *MRS Energy & Sustainability*, vol. 9, no. 2, pp. 198–211, 2022.

[15] M. Amini, M. B. Sanjareh, M. H. Nazari, G. B. Gharehpetian, and S. H. Hosseinian, "A novel model for battery optimal sizing in microgrid planning considering battery capacity degradation process and thermal impact," *IEEE Transactions on Sustainable Energy*, vol. 15, no. 3, pp. 1435–1449, 2024.

[16] A. Maheshwari, N. G. Paterakis, M. Santarelli, and M. Gibescu, "Optimizing the operation of energy storage using a non-linear lithium-ion battery degradation model," *Applied Energy*, vol. 261, p. 114360, 2020.

[17] Y. Wang, C. Zhou, and Z. Chen, "Optimization of battery charging strategy based on nonlinear model predictive control," *Energy*, vol. 241, p. 122877, 2022.

[18] D. I. Stroe, V. Knap, M. Swierczynski, A. I. Stroe, and R. Teodorescu, "Operation of a grid-connected lithium-ion battery energy storage system for primary frequency regulation: A battery lifetime perspective," *IEEE Transactions on Industry Applications*, vol. 53, no. 1, pp. 430–438, 2017.

[19] M. Bueno-Lorenzo, M. Ángeles Moreno, and J. Usaola, "Analysis of the imbalance price scheme in the spanish electricity market: a wind power test case," *Energy Policy*, vol. 62, p. 1010–1019, 2013.

[20] E. Ghanaee, J. I. Pérez-Díaz, D. Fernández-Muñoz, J. Nájera, M. Chazarra, and S. Castaño-Solis, "Optimal scheduling of a hybrid wind–battery power plant in the day-ahead and reserve markets considering battery degradation cost," in *2024 International Conference on Smart Energy Systems and Technologies (SEST)*, 2024.